CLEAVAGE STRESS ON THE DELAMINATION PLANE OF A PLATE STEEL

J. SUN[1] and J. D. BOYD[2]
[1]*Department of Materials Science and Engineering, Xi'an Jiaotong University, Xi'an 710049, P. R. China*
[2]*Department of Materials and Metallurgical Engineering Queen's University, Kingston, Ontario, Canada K7L 3N6*

ABSTRACT

Cleavage fracture stresses, σ_f^*, have been determined on the delamination plane of a plate steel with six different microstructures. Four—point bending was applied on notched specimens. The highest value of σ_f^*/σ_y was obtained for steels having FRT (finish—rolling temperature) between T_{NR} (no—recrystallization temperature) and A_{r3}. For steels rolled in intercritical region (below A_{r3}), the continuous path for cleavage fracture results in the lowest value of σ_f^*/σ_y, related to the smallest P_f/P_{Gr} and X_f/ρ. On the basis of finite element analyses of stress and strain ahead of a notch and of metallographic observation, the deformation history involving the stress triaxiality effect was presented for typical materials at which cleavage fracture initiates. It was revealed that the materials with higher σ_f^*/σ_y experienced larger plastic strains under higher triaxiality.

KEYWORDS

Cleavage fractures stress, material unit, deformation history.

INTRODUCTION

It is well established that thermomechanical processing (TMP) of steel, in particular at low finish rolling temperature (FRT), produces optimum combinations of strength and toughness. However, delamination has been observed in a variety of TMP microalloyed steel plates. The occurrence of delamination has been correlated with reduction in both impact energy (Faucher and Dogan, 1988; Bramfite and Marder, 1977) and the through—thickness strenth of rolled steel plate (Hero et al., 1975). Therefore, with the increased interest in higher strength and toughness of the longitudinal direction, more attention is being paid to the consideration of through—thickness strength and toughness of rolled steel plate (Fegredo, 1975; Dogan and Boyd, 1990) because of lamellar tearing in heavy—section, welded structures, notable offshore drilling platforms.

The fracture mode of delaminations is mainly brittle cleavage (Engl and Fuchs, 1982; Brozzo and Buzzichelli, 1977) and follows a critical cleavage fracture stress criterion in the through-thickness direction (Kuhne et al., 1982; Baldi and Buzzichelli, 1978). The cleavage fracture stress is anisotropic for controlled rolled plate. Recently, quantitative research showed (Sun and Boyd, 1994) that the anisotropy of cleavage fracture stresses increases with decreasing

FRT and is related to their microstructures. However, in through—thickness direction, the highest cleavage fracture stress is always achieved by plates finished—rollled below T_{NR} but just above A_{r3}, even though the highest value of σ_f^* is only 85% of longitudinal one. Furthermore, it is necessary to know if the through—thicknes cleavage fracture stress of rolled plates could be improved considerably by suitable rolling schedues combined with some cooling way after rolling and how the cleavage fracture stress is affected by microstructures of rolled plates.

In general, it is reasonable to consider that there was a relationship, similar to Hall—Petch mode, between the values of σ_f^* and the sizes of ferrite grains in steel (Smith, 1966). In further investigation of critical events in cleavage fracture of steels, however, it was revealed that σ_f^* is more regularly related to the sizes of the terrace characterizing the dimension of ferrite cracks than that of ferrite grains directly (Chen et al., 1991). Recent results (Chen et al., 1994) suggested a criterion composed of three items for cleavage fracture, i. e. the plastic strain $\varepsilon_P = \varepsilon_{PC}$ for initiating a crack nucleus; the stress triaxiality constraint $\sigma_m/\bar{\sigma} \geqslant (\sigma_m/\bar{\sigma})_C$ for preventing the crack nucleus from blunting; and $\sigma_{yy} \geqslant \sigma_f^*$ for propagating the crack nucleus into a critical size. It would also be of interest to study the variation in σ_f^* with microsructures based on the deformation history and failure locus of material units along this line.

The aim of the project reported here is to investigate quantitatively the effect of different rolled microstructures on the through—thickness cleavage fracture stress of the steel plate and try to evaluate the acceptibility of thermomechanical processing parameter in the production of delamination—resistant steel plates for some specific application.

EXPERIMENTAL

Materials

A microalloyed Ti—V—N steel plate was used with a thickness of 25mm, which is a typical one for offshore application. The composition of the steel is given in Table I. The experimen

Table I Composition of Experimental Steel (Weight Percent)

C	Mn	Si	S	P	Al	Ti	V	N	O
0.08	1.26	0.29	0.005	0.003	0.04	0.01	0.08	0.012	0.009

tal steel plates were produced by rolling slabs of this steel by three different rolling schedules (finish rolling temperature FRT = 950℃, 830℃, and 700℃; i. e., completely recrystallized rolling, non—recrystallized rolling, and intercritical rolling respectively), followed by either air cooling or water quenching. Six different microstructures were produced by the thermomechanical processing conditions above and referred as B1, B2, —, B6 respectively. A detail description of the processing and microstructures of the plate was given by Dogan et al., (1988).

Specimens

All specimens were single—edge—notched and tested in four—point bending (4PB) at —196℃ on an Instron Universal Testing Machine with a crosshead speed of 0.5mm/min. They

were all of through thickness orientation, i. e., the fracture plane was parallel to the rolling plane, and crack propagation was in the longitudinnal direction. Stubs were friction welded on the plate for the through—thickness samples. The specimen was 8 mm square bar with a notch, located at mid—thickness plane of the plates, of 3mm deep, 45 deg flank angle and a notch radius of $\rho = 0.25$mm. The fracture surface of each fractured sample was examined by SEM. A few of double notched 4PB samples (DNB) was used to observe the non—propagating microcracks ahead of the uncracked notch.

Calculations of Stress and Strain Distributions

An elastic—plastic finite element program was employed to calculate the distributions of stress, strain and stress triaxiality ahead of a notch. The complete description of the FEM calculation has been presenttd in earlier research (Yan et al., 1993). The calculation was repeated for each fractured specimen from elastic regime until general yield. From the results, the deformation history of material units at cleavage initiation position could be obtained by seting the values of the measared X_f/ρ and the fracture load, (P_f/P_{GY}).

Determination of Cleavage Stress σ_f^*

In order to measure σ_f^* accurately, the distance from the notch root to the cleavage fracture site (X_f) was determined by the SEM on the fracture surface of every single—notch 4PB specimen. From the stress distribution curve corresponding to the fracture load, the local normal stress at distance X_f could be obtained and was taken as the cleavage fracture stress σ_f^*.

RESULTS

Microstructural Parameters

The microstuctures of the plates have been described elsewhere (Dogan et al., 1988). The results of the guantitative metallography measurements for six plates are reported in Table Ⅱ.

Table Ⅱ Microstructures and Room—Temperature Yield Strength of TMP Plate

Plate	FRT/Cooling	F(%)	DF(%)	P(%)	B+M(%)	D(μm)	σ_y(MPa)
B1	950/AC	87.9		12.1		31.4	283.0
B2	950/WQ	69.8		3.0	27.2	20.7	443.0
B3	830/AC	90.2		9.0	0.8	15.2	334.0
B4	830/WQ	66.1		6.8	27.1	14.8	382.0
B5	700/AC	34.5	54.6	9.8	1.1	11.3	448.0
B6	700/WQ	24.3	62.2		13.5	10.7	505.0

F=Polygonal Ferrite; DF=Deformed F; P=Pearlite; B=Bainite; M=Martensite; D=F Grain Diameter

The aveavage ferrite grain diameter, D, was determined by an Image Analyzer.

Distributions of Stress and Strain

Figure 1 shows the stress and strain distributions, calculated by finite element method, ahead of a notch, where P is the applied load, P_{GY} is the general yield load, X is the distance to

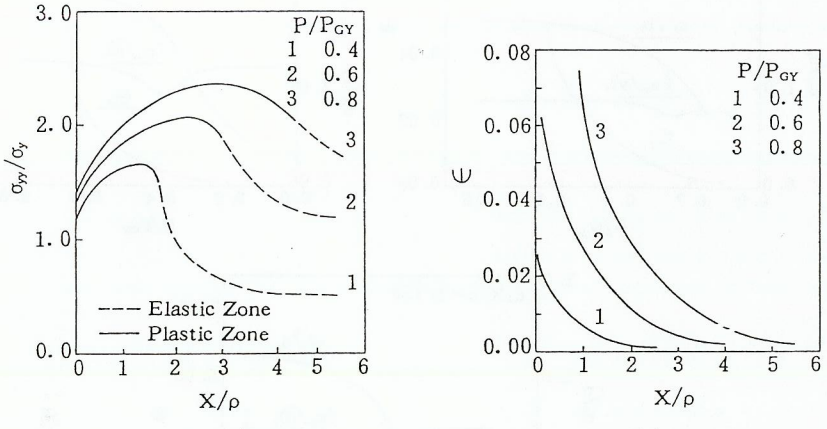

Fig. 1—(a) Stress and (b) strain distributions dhead of the notch.

notch root. In Fig. 1, with increasing the load, (P/P_{GY}), the normal stress σ_{yy} and effective strain ε_{eff} increase, and the peak of the σ_{yy} moves away from the notch root. Figure 2 illus-

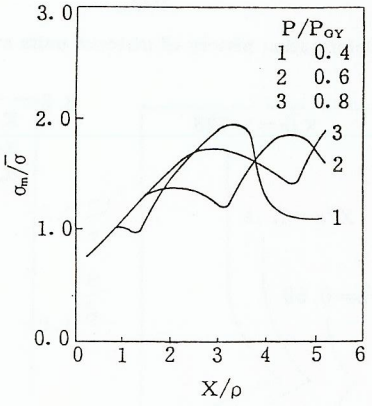

Fig. 2—Distribution of stress triaxiality ahead of the notch.

trates the variation of stress triaxiality $\sigma_m/\bar{\sigma}$ with the applied load, (P/P_{GY}), which is considerablly different from those of σ_{yy} and ε_{eff} above. At a lower applied load, the value of $\sigma_m/\bar{\sigma}$ increases with X/ρ and has a peak far away from the notch root. With increasing the load, a

plastic zone appears and spreads out gradually. At the boundary of the plastic zone, the triaxial constraint is relaxed somewhat so that $\sigma_m/\bar{\sigma}$ has a minimum value there and two peak values, lower one in the plastic zone.

Cleavage Fracture Stress

The measurements of the through—thickness cleavage fracture stress σ_f^* for the six plates are given in Fig. 3. Generally σ_f^* of WQ plate is higher than that of its AC counterpart individual

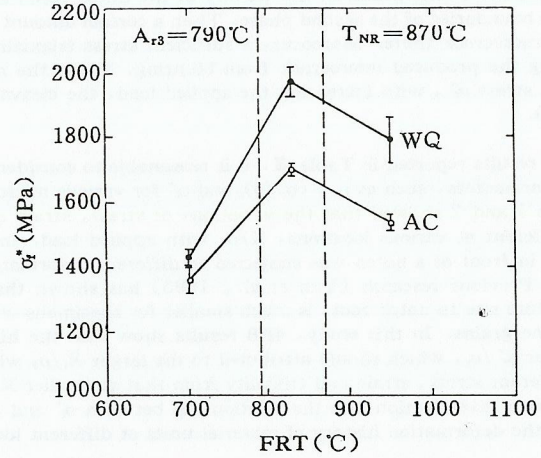

Fig. 3—Variation of σ_f^* with FRT.

Table Ⅲ Results of 4PB Test at −196℃

plate	σ_y(MPa)	P_f/P_{GY}	X_f/ρ	X_{max}	σ_f^* (MPa)	σ_f^*/σ_y	ε_{fc}	$(\sigma_m/\bar{\sigma})_{fc}$
B1	773	0.606	1.61	2.13	1537.52±24.39	2.00	0.018	1.31
B2	958	0.569	1.18	2.05	1790.00±71.72	1.88	0.023	1.19
B3	817	0.704	1.30	2.51	1701.26±18.43	2.09	0.033	1.25
B4	909	0.813	1.73	2.92	1971.86±46.86	2.18	0.035	1.43
B5	905	0.379	0.51	1.17	1362.93±44.03	1.51	0.013	0.87
B6	955	0.402	0.50	1.27	1429.31±26.90	1.49	0.012	0.85

ly becuase of refinement of ferrite grains in WQ plate and the presence of banded pearlites in AC plate. For each same cooling treatment, either AC or WQ respectively, σ_f^* is lowest for plate rolled below A_{r3}, which contain heavily banding structures, and the highest value of σ_f^* was obtained from plate, non—recrystallization rolled, containing about 30% bainite (+ martensite) distributed uniformly in the matrix of about 70% refined ferrite. The optimum

value of σ_f^* was presented by plates finish—rolled about mid—section between T_{NR} and A_{r3} followed by water quenched. Also, the results of 4PB tests are given in Table Ⅲ. The avearage value of 4～5 samples has been taken as P/P_{GY}, X_f/ρ, X_{max}/ρ, ε_{fc}, and $(\sigma_m/\bar{\sigma})_{fc}$ for B1, B2, ……, B6 respectively. It is indicated from SEM observations on fracture surfaces of samples that the distance X_f, cleavage initiation site, is always smaller than X_{max}, i. e. , cleavage fracture occurs in the left side of the location for σ_{max}.

DISCUSSION

The process of the cleavage fracture has been described as follows: when the applied load is increased, slips occur in the grains in the vicinity of the notch root, and dislocations move and pile up at the boundaries of the second phase. Then a certain amount of plastic strain is needed to initiate a microcrack there. Moreover, a sufficient stress triaxiality constraint is necessary for preventing the produced microcrack from blunting. When the normal stress exceeds the local fracture stress σ_f^*, with increasing the applied load, the cleavage fracture occurs (Chen et al. , 1994).

Based on the results reported in Table Ⅲ. it is reasonable to consider that there should be different local parameters, such as ε_{pc}, $(\sigma_m/\sigma)_c$ and σ_f^* for various microstructures. On the other hand, Figure 1 and 2 showed that the variations of stress, strain and triaxiality ahead of a notch are different at various locations, X/ρ, with applied load. In other words, individual material unit in front of a notch was subjected to different deformation process dependent on the location. Previous research (Yan et al. , 1993) has shown that the X_f, distance from cleavage fracture site to notch root, is much smaller for specimens with coarse grains than for those with fine grains. In this study, 4PB results show that the higher P_f/P_{GY} is associated with its higher σ_f^*/σ_y, which should attributed to the larger X_f/ρ, where the material unit experienced different stress, strain and trixiality from that at smaller X_f/ρ. Therefore, it is necessary to make a investigation into the relationship between σ_f^* and microstructures from the viewpoint of the deformation history of material units at different location ahead of a notch.

From the results presented in Table Ⅲ, the plates B2, B4 and B6 have been taken as examples with the X_f/ρ of 1. 18, 1. 73 and 0. 5 respectively. The σ_{yy}/σ_y, $\sigma_m/\bar{\sigma}$ and ε_{eff} were plotted againest the applied load, P/P_{GY} in Fig. 4 for material units located at X/ρ=1. 18, 1. 73 and 0. 5 corresponding to the situations of plates B2, B4 and B6 individually. With increasing the applied loads at 3 points, the principal stress and effective strain increase and eventually exceed the critical fracture stress and strain whereas the triaxial constraint varies as butterfly—like with a bottom value at a point of yielding strain and remains approximately constant as the applied load is further increased. That is to say that different stress and strain have benn experienced for each material unit located at various X/ρ, or for different plates. Figuer 5 shows the ε_{eff} and $\sigma_m/\bar{\sigma}$ values at the measured cleavage initiation positions with X/ρ of 1. 18, 1. 73 and 0. 5 for three plates. They represent the critical strain for initiating a crack nucleus and the critical triaxiality of stress for preventing the crack nucleus from blunting respectively. It can be seen that, even under a higher triaxial constraint, the material unit at X/ρ=1. 73 for B4 plate has a larger critical strain than that for B2 plate under lower triaxiality. The smallest critical strain is obtained by material unit at X/ρ=0. 5 for B6 plate under the lowest triaxiality. Consequently, it can be concluded that higher σ_f^*/σ_0 was obtained by plates with larger X_f/ρ, which could not be reached by plates with smaller X_f/ρ. as indicated in Fig. 6, in which, the variations of σ_{yy}/σ_y and $\sigma_m/\bar{\sigma}$ with a applied load were presented for material units at different locations of X_f/ρ.

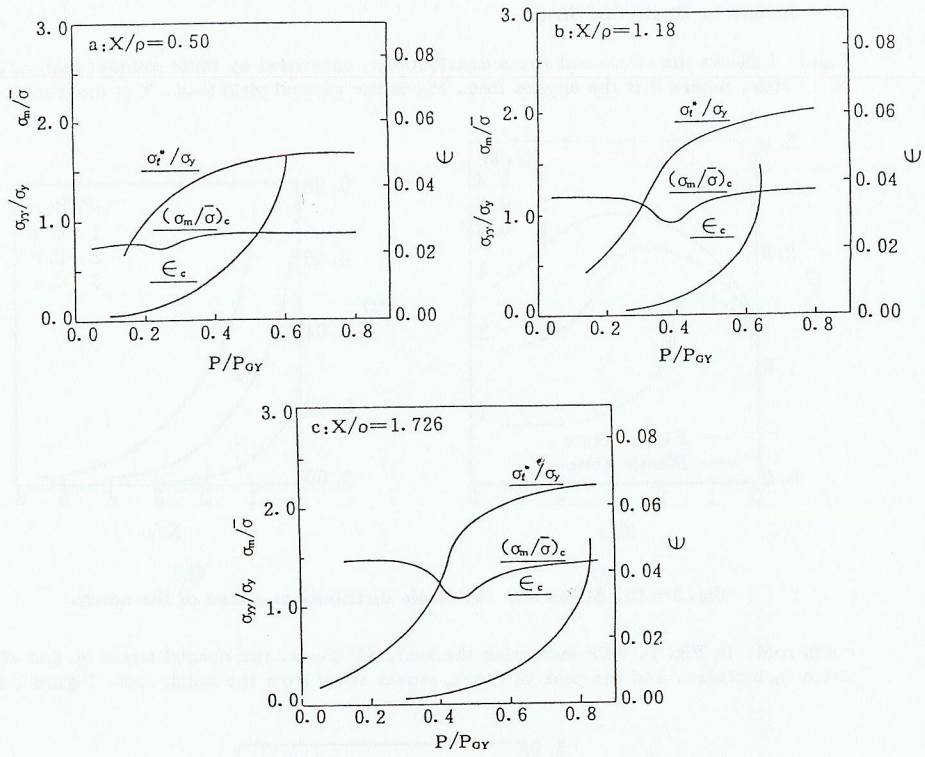

Fig. 4—Deformation history of material units at different locations.

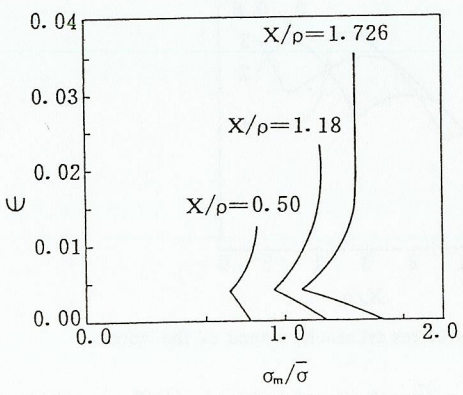

Fig. 5—Strain and triaxiality of material units at cleavage initiation sites.

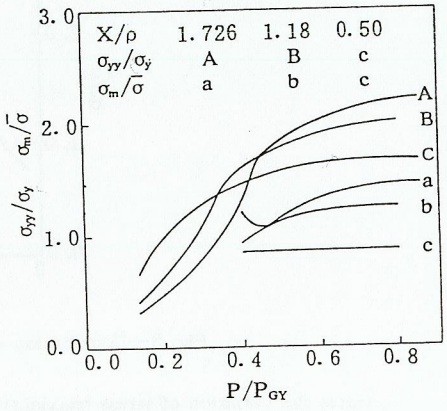

Fig. 6—Variations of σ_{yy}/σ_y and $\sigma_m/\bar{\sigma}$ with applied load for different material units.

In summary, for the plates with larger X_f/ρ, the material units at cleavage initiation site have greater critical plastic strain even under higher triaxial constraint, which contributes directly to the higher σ_f^*/σ_y. That is to say that the resistance of steel plates to delamination has been much improved by the processing with FRT above A_{r3}.

CONCLUSION

The highest values of σ_f^* are found for steels having FRT (finish—rolling temperature between T_{NR} (no—recrystallization temperature) and A_{r3} (start of PF transformation), and the lowest values of σ_f^* are obtained when FRT is below A_{r3}. Steels having FRT above T_{NR} exhibit intermediate values of σ_f^*. The values of σ_f^* for water—quenched plate are constantly higher than for the corresponding air cooled plate because of smaller ferrite grain size. At the cleavage initiation site ahead of a notch, the samples experienced larger plastic strains under higher triaxiality for plates with higher σ_f^*/σ_y than those with lower σ_f^*/σ_y.

ACKNOWLEDGMENTS

The authors gratefully acknoweldge research support from NSERC Canada and NNSF China.

REFERENCES

Baldi, G. Buzzichelli, G. (1978). Critical stress for delamination fracture in HSLA steels. Metal Science, 12, 459—472.

Brozzo , P. Buzzichelli, G. Mascanzoni, A. and Mirable, M. (1977). Microstructure and cleavage resistance of low—carbon bainitic steels. Metal Science, 11, 123—129.

Bramfite, B. L. and Marber, A.R. (1977). Metall. Trans. A, (1977). 8A, 1263—1273.

Chen, J. H. Zhu, L. Wang, G. Z. and Wang, Z. (1991). Further investigation of critical events in cleavage fracture of C—Mn base and weld steel. Metall. Trans. A, 24A, 659—667.

Chen, J. H. Yan, C. and Sun, J. (1994). Further study on the mechanism of cleavage fracture at low temperatures. Acta metall. mater. 42, 1, 251—261.

Dogan, B and Boyd, J. D. (1990). Through—thickness fracture of a Ti—V—N plate Steel. Metall. Trans. A, 21A, 1177—1191.

Engl, B. and Fuchs, A. (1982). The cause of separations and its effects on fracture behaviour. In: Proc. 4th Eur. conf. on Fracture, pp. 335—342 Chameleon Press, London.

Faucher , B. and Dogan, B. (1988). Evaluation of the fracture toughness of hot—rolled low—alloy Ti—V plate steel. Metall. Trans. A, 19A, 505—516.

Fegredo, D. M. (1975). Can. Metall. Quart., 14, 243—255.

Hero, H. Evensen, J. and Embury. J. D. (1975). Can. Metall. Quart., 14, 117—122.

Kühne , K. Dunnewald, H. Dahl, W. (1982). Reasons for the appearance of separations in HSLA—steels. In: Proc. 4th Eur. Conf. on Fracture, pp. 329—334, Chameleon Press, London.